



Laying out the foundations: Assessing the spatial extent and drivers of offshore wind turbine artificial reef effects on soft sediments

Nene Lefaible^a, Carl Van Colen^{a,*}, Christelle Jammart^a, Jan Vanaverbeke^{a,b}, Tom Moens^a, Sven Van Haelst^c, Alain Norro^b, Steven Degraer^{a,b}, Ulrike Braeckman^{a,b}

^a Marine Biology Research Group, Ghent University, Krijgslaan 281, S8, 9000 Gent, Belgium

^b Institute of Natural Sciences, Operational Directorate Natural Environment, Marine Ecology and Management, Vautierstraat 29, 1000 Brussels, Belgium

^c Flanders Marine Institute (VLIZ), Jacobsenstraat 1, 8400 Oostende, Belgium

ARTICLE INFO

Keywords:

Offshore renewable energy
Spatial reef effects
Macrobenthos
Biological trait analysis
Ecosystem functioning

ABSTRACT

With the rapid expansion of offshore energy, numerous artificial structures are being installed on the seabed, including wind turbine foundations. This study investigates the “artificial reef” (AR) effect of bottom-fixed offshore wind farms (OWFs) on soft sediment benthic communities. While previous studies have focused on distances ≥ 30 m from turbines, in this study, sediment and macrobenthic samples were collected at shorter distances (1 m, 7 m, 15 m and 25 m) from the scour protection layer (SPL) around a monopile and a gravity-based foundation in two Belgian OWFs, 10–13 years post-installation. Results show a localized AR footprint for both turbine foundations, with enriched benthic communities within 15 m of the SPL. In comparison to communities 25 m distanced away from the SPL, a higher average species richness (+100 %), abundance (+117 %), functional richness (+438 %), and bioturbation potential (+86 %) was prevalent, whereas the magnitude of enriched structural and functional diversity in the footprint varied respectively between 16 and 80 % and 15–110 % depending on the OWF. Beyond the AR footprint, communities resembled those at reference sites (240–570 m), with less surface dwellers, suspension feeders and a prevalence of burrowing bioturbators that contribute little to bioturbation. While the AR effect’s magnitude depends on local conditions and foundation design, our trait-based analysis indicates that sediment fining, biofouling drop-offs and organic enrichment are consistent drivers shaping the AR footprint.

1. Introduction

Since the construction of the first offshore wind farm (OWF) in Denmark during the 1990’s, rapid OWF expansion has occurred in European waters in order to become climate neutral by 2050 in light of the “Green Deal” (deCastro et al., 2019). Moreover, supplementary targets were recently set during the 28th Conference of the Parties climate summit in Dubai (COP28), where nearly 200 countries agreed to triple renewable power and enhance its efficiency by 2030 (www.irena.org). These ambitious initiatives and increased investments of non-European countries such as China and the United States denote that the global energy transition is gaining momentum. The infrastructure capacity to achieve these objectives (e.g., bottom-fixed and floating turbines, floating solar panels and tidal energy systems) requires substantial ocean space and implies an extensive introduction of artificial hard substrates at sea. In parallel, potential ecological footprints of this sector

on the marine environment have been investigated (Galparsoro et al., 2022; Vaissière et al., 2014). An important scientific finding is that the submerged parts of OWF structures (i.e., turbine foundation, scour protection layer), act as “artificial reefs” (AR) with a rapid colonization by hard-substrate species after installation with an overall increase in biodiversity (Dannheim et al., 2020; Degraer et al., 2020; Galparsoro et al., 2022; Vivier et al., 2021; Zupan et al., 2023). In addition, because fishery activities are often prohibited in OWF sites, these sites function as potential refuge areas for commercially exploited species (Buyse et al., 2023; Prusina et al., 2020; ter Hofstede et al., 2022; Vivier et al., 2021).

To amplify the so called AR-effect, OWF companies now explore integrated approaches such as nature-inclusive designs (Glarou et al., 2020; Kingma et al., 2024; Pardo et al., 2025; Rendle et al., 2023; Vivier et al., 2021). For example, some countries are introducing new permit obligations that require demonstrable efforts to maximise conservation

* Corresponding author.

E-mail address: carl.vancolen@ugent.be (C. Van Colen).

<https://doi.org/10.1016/j.seares.2025.102631>

Received 4 June 2025; Received in revised form 15 September 2025; Accepted 18 September 2025

Available online 23 September 2025

1385-1101/© 2025 The Authors. Published by Elsevier B.V. This is an open access article under the CC BY-NC-ND license (<http://creativecommons.org/licenses/by-nc-nd/4.0/>).

efforts such as eco-friendly scour protection designs (Kingma et al., 2024; Prusina et al., 2020). These ecological “benefits” are accompanied by increased public acceptance of OWFs and are often used at a governance level to justify and promote the further expansion of marine infrastructure. On the other hand, this has created a bias within currently available literature with a stronger research focus on hard-substrate-associated species such as epifaunal communities and fish, while other ecosystem components adjacent to the turbine foundations (e.g., hyperbenthos and infauna of mobile sediments, such as macrobenthos) remain rather understudied (Galparsoro et al., 2022). Investigating benthic habitats is further complicated by aspects such as rough weather conditions and safety regulations nearby the structures, resulting in a limited number of samples taken at short distances from the structures and the general perception that AR effects on surrounding benthic habitats are minimal (Zucco et al., 2006; Jak and Glorius, 2017).

A combination of physical and biological pressures associated with the overarching AR effect is expected to influence surrounding sediments through different mechanisms (Coates et al., 2014; Dannheim et al., 2020; Degraer et al., 2020; Hutchison et al., 2020; Lefaible et al., 2023; Jammal et al., 2025). Firstly, modified subsurface current flows around the structures create complex sediment transport processes (Baeye and Fettweis, 2015; Brandao et al., 2023; Chen et al., 2014; Fettweis et al., 2022; Floeter et al., 2017; Miles et al., 2017). Secondly, most of the established epifaunal fauna on the turbine foundations (e.g., mussels, tube-building amphipods and anemones) capture and ingest particles suspended in the water column (Mavraki et al., 2020), thereby affecting local primary production and flow of organic matter to the seabed through bio-deposition of faecal pellets and detritus (Mavraki et al., 2022; Voet et al., 2023). Additionally, the manifestation of dropped off epifauna (“biofouling drop-off”) on the seabed can cause a local expansion of the AR through their habitat modifying properties (Degraer et al., 2020; Hutchison et al., 2020; Lefaible et al., 2023).

The few available studies on soft sediments confirm that AR habitat alterations lead to shifts in benthic distributions (Coates et al., 2014; Hutchison et al., 2020; Lefaible et al., 2023). Sediments in the immediate surrounding of the turbine foundations were generally characterized by enhanced accumulation of finer-grained material with enriched infaunal communities showing higher abundances and diversity (Coates et al., 2014; Hutchison et al., 2020; Lefaible et al., 2023; Jammal et al., 2025). Next to benthic enrichment, communities were composed by more nearshore species and habitat-forming species such as the sand mason, *Janice conchilega* (Coates et al., 2014; Lefaible et al., 2023). However the intensity and spatial extent of AR effects vary considerably, probably depending on site-specific aspects such as foundation type and natural conditions (e.g., water depth, hydrological regime, sediment composition) (Coolen et al., 2022; Lefaible et al., 2023; Jammal et al., 2025). Furthermore, it is unknown how turbine foundation presence will influence seabed functions and processes, such as nutrient cycling and sediment reworking, through change in functional composition of benthic communities (Degraer et al., 2020). Recently, studies using functional diversity indices and biological trait analysis (BTA) as proxies for ecosystem functioning were instrumental in linking habitat modifications resulting from human activities with functional responses of soft-sediment benthic communities (Bolam et al., 2016; Festjens et al., 2023; Goedefroo et al., 2023). Similar applications to assess the functional implications of the AR effect on marine biota exist (Gutow et al., 2014; Boutin et al., 2023; Kingma et al., 2024), but are scarce for infaunal communities.

To address these knowledge gaps, our study compared small-scale structural and functional changes in the macrobenthos community in the close vicinity of a gravity-based and monopile foundation and their SPLs, situated in two Belgian OWFs. The foundations differ in terms of environmental conditions such as distance from the coastline, hydrodynamic regime and sediment characteristics (e.g., granulometry, food availability) and their SPL varies in surface. Sediment and macrobenthic samples were collected at four distances within the 25 m range from the

SPLs along the main axis of deposition in the residual tidal current direction, where most benthic change is expected (Coates et al., 2014). Besides structural properties (i.e. total abundance, biomass, diversity and community composition), functional diversity indices and the bioturbation potential (BPC) were included in the infauna community analysis. Biological trait analysis (BTA) was also performed, where a distinction was made between “response traits” that are directly associated with occurring pressures such as living habitat and mobility, and “effect traits” (e.g., bioturbation, feeding mode) that can affect ecosystem functioning indirectly (Bolam et al., 2016, 2023). We hypothesized that the spatial extent of the AR benthic footprint would differ between sites due to varying local environmental conditions, such as the position of the turbine foundation on the sandbank. Furthermore, by applying a biological trait analysis (BTA) we aimed at gaining mechanistic insights into the benthic AR response and its possible effects on benthic ecosystem functioning.

2. Material and methods

2.1. Study area

The eastern OWF concession zone (238 km²) in the Belgian part of the North Sea (BPNS) has been allocated for the development and production of offshore renewable energy. Today, 399 turbines are operational within nine operational OWFs, installed between 2009 and 2020 at distances ranging from 23 to 54 km from the coastline (<https://www.belgianoffshoreplatform.be>).

2.1.1. OWF sites and foundations

The monopile foundation (MP, coded D08) under study is positioned at 19 m depth in the central part of the Belwind OWF on the crest of the Hinderbanken, located at 49 km offshore (Fig. 1). The Belwind OWF became fully operational in 2010 and comprises a total of 55 monopiles, which are steel piles with a diameter of 5 m (<https://www.belgianoffshoreplatform.be>). The C-Power OWF is located at ~30 km offshore and is divided into two sub-areas. The gravity-based foundation (GBF, coded D05) investigated in this study is situated at 21 m depth at the slope of the Thornton bank in the middle of a row of six GBF turbines in the western sub-area that were constructed during phase I of the C-Power project, which was operational in 2009 (Fig. 1). Since 2010, these GBF turbines are surrounded by 48 jacket foundations (<http://www.c-power.be>). (Fig. 1)

GBFs are concrete, hollow structures, comprised of a pile (ϕ 6.5 m) that merges into a conical bottom section (ϕ 6.5 m – 23.5 m), placed on a foundation basis (i.e., filter and gravel layer) on the seabed. Monopiles consist of steel cylinders (ϕ 5 m), with different length, depending on the water depth and capacity. A scour protection layer (SPL) is placed at the base of both MP and GBF to prevent scouring around the structures. SPL are mainly composed of an armour layer of rocks with varying crest diameters depending per turbine foundation type (D08: 33 m and D05: 51 m) (Fig. 1). This armour layer overtops the filter layer (14 m and 55.5 m diameter for D08 and D05, respectively) which consists of pebbles. The surface area of the SPL for MP D08 is thus 134 m², while that of the GBF D05 is 1609 m². The foundation and SPL of D08 and D05 are both fully colonised by hard-substrate fauna. Succession patterns in the colonization of the turbine foundation are described by Kerckhof et al. (2010) and Zupan et al. (2023), while De Mesel et al. (2015) further discuss the subtidal and intertidal samples collected along the foundation structure. The mobile sands move also within the SPL, so the filter layer of the SPL is also covered with sand.

2.1.2. Reference conditions

Both OWF sites are located on subtidal sandbanks (Belwind: Hinder Banken, Bligh Bank; and C-Power: Zeeland Banken, Thornton Bank), in an area where west-southwest winds and a semidiurnal tidal current regime oriented along the northeast-southwest axis, prevail (Baeye and

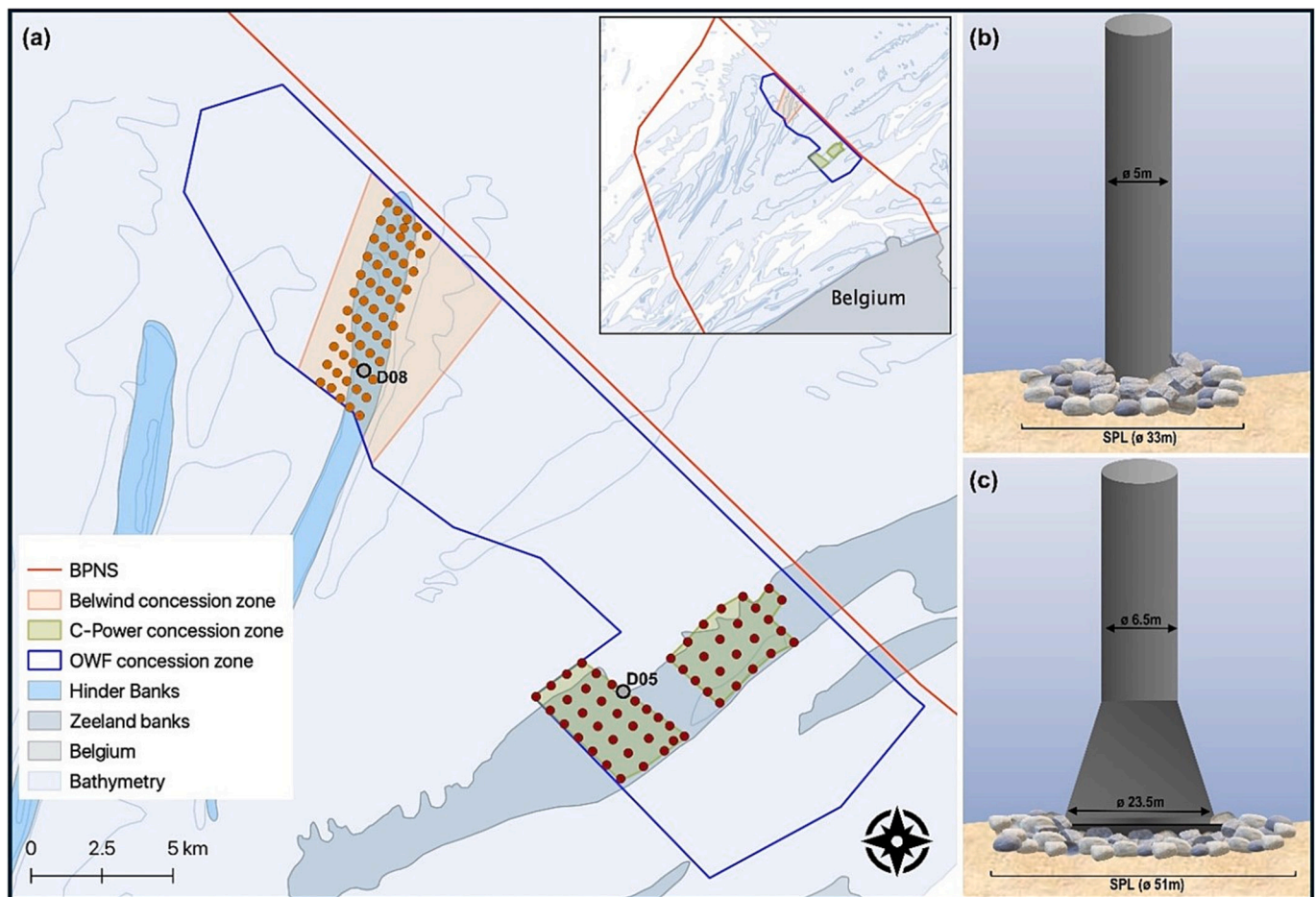


Fig. 1. (a) Location of the turbines under study in the offshore windfarms (OWFs) Belwind (D08) and C-Power (D05) within the eastern concession zone of the Belgian Part of the North Sea. Schematic representation of the (b) monopile foundation and (c) gravity-based foundation, with corresponding diameter (ϕ) specifications of the piles and scour protection layers (SPLs).

Fettweis, 2015). The more offshore located Bligh Bank receives clear and less productive water masses from the English Channel, while Thornton Bank is situated in the convergence zone between the English Channel and turbid, well-mixed coastal water masses (Fettweis et al., 2022; Lacroix et al., 2004). Reference conditions for each location were determined during post-construction monitoring studies, in which samples were collected at distant positions (i.e. 240–570 m) from the turbine foundations within each OWF (Lefaible et al., 2023).

Corresponding ecological properties based on five year of data (Autumn 2015–2019, C-Power $n = 130$, Belwind $n = 135$) of 0.1 m² Van Veen grab samples are summarized in Supplementary Table 1 and revealed that the C-Power OWF site harbors finer sediments with higher food availability in terms of sediment organic matter compared to the Belwind OWF site (Supplementary Table 1). Sediments at both sandbanks are considered permeable with poor stratification of organic matter due to the advective porewater flows regularly flushing the interstitial spaces (Huettel et al., 2014). Biological characteristics corresponded with the *N. cirrosa* and *H. elongata* communities, which naturally occur within both sandbank systems (Breine et al., 2018). These offshore communities are predominantly composed of polychaete and amphipod species (e.g., *Nephtys cirrosa*, *Spio* sp., *Bathyporeia elegans* and *Urothoe brevicornis*), with low to moderate abundances (< 450 ind. m⁻²) and diversity (species richness < 10 spp.sample⁻¹ and Shannon-diversity < 1.85) (Supplementary Table 1). These reference data were used for a posteriori comparisons with this study's samples collected in the vicinity of the SPL.

2.2. Sample collection

All samples were obtained on board of the RV Simon Stevin and RV Belgica by a team of occupational scientific divers (Féral and Norro, 2023) operating from a RHIB in August 2020 (Belwind) and September–October 2022 (C-Power). Sampling occurred along the south-west (SW) axis adjacent to the SPL of D05 and D08 (Fig. 2). This axis was chosen as it aligns with the residual NE current direction where strongest deposition effects are expected and where biological enrichment was observed before (Coates et al., 2014). Two scientific divers descended along the turbine and swam to the edge of the SPL on the SW-side. One diver attached a tape measure to the edge of the SPL and started swimming away from it, following a SW bearing on their compass and simultaneously unrolling the tape measure. The second diver followed along the tape measure and took the sediment cores while hovering over the sediment surface. Samples were taken randomly taken within the diver's arm reach at four distances relative to the edge of the SPL at D08 (Belwind; 1 m, 7 m, 15 m and 25 m), while sampling was restricted to three distances (C-Power; 7 m, 15 m and 25 m) at D05 due to logistical reasons (Fig. 2).

Six 25 cm long sediment cores (ϕ 3.6 cm) were collected at each sampling location, which was the maximum number possible during the one hour diving window. For each sampling location, three sediment cores were stored separately for further granulometric analysis in the laboratory. Two subsamples were taken from the first 0–5 cm sediment depth layers from the other sediment cores using cut-off syringes (10 ml), wrapped in aluminum foil and stored at -20 °C for total organic

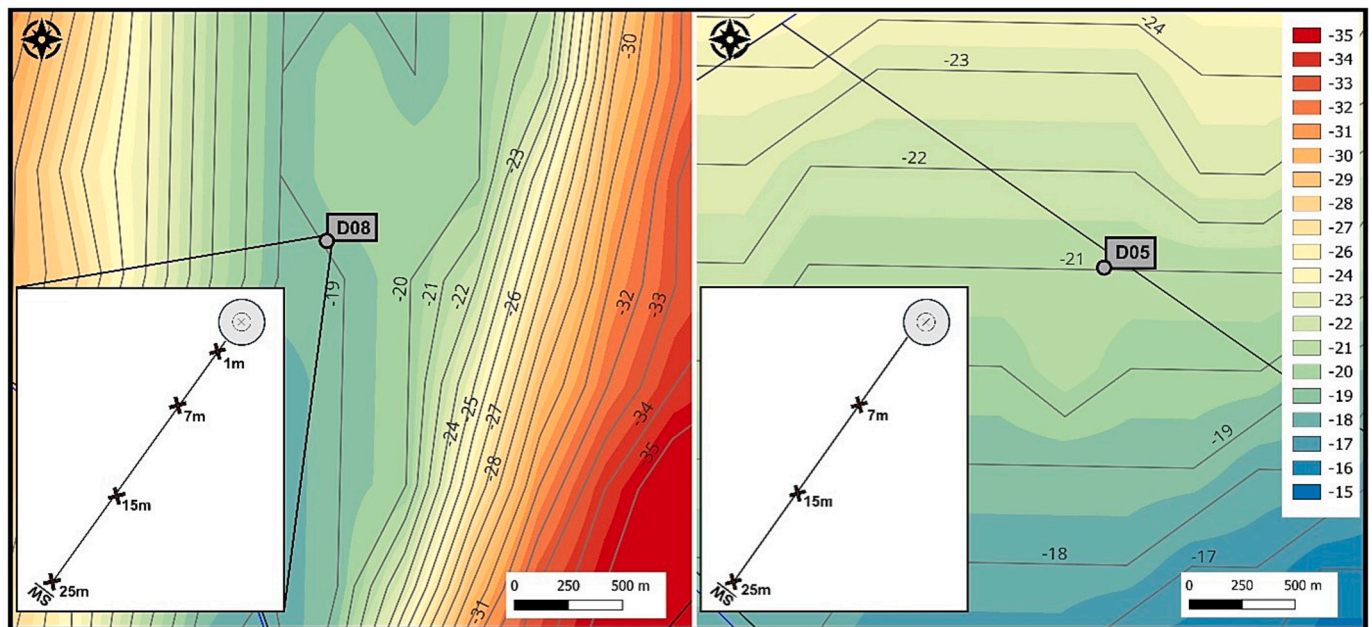


Fig. 2. Bathymetric map with water depth contour lines, depicting the location of the monopile (D08, Belwind windfarm) and gravity-based (D05, C-Power windfarm) foundations. Left insert shows the sampling strategy with black crosses representing the sampling distances (1 m–25 m) along the south-west axis of the turbine foundation.

carbon (TOC %) and pigment measurements. Back in the laboratory, samples for pigment analysis were stored at -80°C until extraction. Subsequently, sediment samples were freeze-dried and homogenized, and a subsample was analyzed for Chlorophyll-a content by HPLC (Gilson) analysis according to Wright and Jeffrey (1997). Another subsample was decalcified with 37 % HCl, and total organic carbon (TOC) was measured using a Flash 2000 NC Sediment Analyzer (Interscience). Macro-benthic sample collection was performed by means of open, metal frames (0.1 m^2) which were pushed into the seabed ($\sim 10\text{ cm}$). The complete sediment content of the frame sample was collected in bags (mesh size of 1 mm) using an airlift pump device and immediately sieved on board (1 mm mesh-size sieve) and preserved in a 4 % formaldehyde-seawater solution. Three replicates were taken at each sampling distance, except for the 15 m sampling position at the Belwind OWF where only two replicates could be collected, leading to a total of 20 macrofaunal samples (Belwind $n = 11$ and C-Power $n = 9$) (see Table 1).

2.3. Sample processing

2.3.1. Biological variables

Macro-benthos samples were first stained with Rose Bengal and organisms were separated from the sediment through a repeated decantation over a 1 mm sieve. The remaining samples were sorted, counted and identified to the lowest possible taxonomic level, using a stereo

Table 1

Sample collection overview with the number of replicated macrofauna and environmental samples around D08 and D05.

| Sampling distance | Monopile foundation, D08 (August 2020) | | Gravity-based foundation, D05 (September–October 2022) | |
|-------------------|--|---------------|--|---------------|
| | Macrofauna | Environmental | Macrofauna | Environmental |
| 1 m | 3 | 6 | / | / |
| 7 m | 3 | 6 | 3 | 6 |
| 15 m | 2 | 6 | 3 | 6 |
| 25 m | 3 | 6 | 3 | 6 |
| Total # samples | 11 | 24 | 9 | 18 |

microscope. In case of uncertain identification, taxa were lumped to genus level. Two structural diversity indices were calculated: species richness (S) and Shannon-Wiener diversity (H'). Biomass (g) was determined for each taxon as blotted wet weight per sample. Macrofaunal counts and biomass per sample were converted to total abundance and biomass (TN, ind. m^{-2} and TB, g m^{-2} ; respectively).

2.3.1.1. *Biological trait score matrix.* The functional composition of benthic communities can be described using biological traits (i.e. species-specific physiological, morphological, behavioural and other relevant biological attributes in a community, sensu Bremner et al., 2006). These traits can be mapped in a biological trait analysis (BTA).

A total of ten biological traits was chosen which can be divided into response traits (mobility, morphology, living habitat, sediment position, egg development) and effect traits (bioturbation, maximum body size, feeding mode, maximum longevity, larval development) (Bolam et al., 2016)(Supplementary Table 2). Each species was assigned to categories of a biological trait, applying a fuzzy coding method with scores ranging from 0 (no affinity) to 1 (high affinity), based on an adapted dataset of Breine et al. (2018). Affinities with multiple categories were possible, but the total sum of the scores always equaled 1. Scores were not available for the groups Bivalvia juvenile, Decapoda juvenile and Nemertea, which comprised 0.2 %, 6 % and 3 % of the total abundances within the entire dataset. Consequently, these taxa were excluded from the final species-trait score dataset.

2.3.1.2. *Functional indices.* Functional diversity indices can be calculated based on a species traits and corresponding abundances. These indices represent independent measures of functional trait space and how species are dispersed within this trait space (Festjens et al., 2023 and references therein).

Functional diversity (FD) indices were quantified for each sample using the FD software of Laliberté and Legendre (2010), with the species-trait matrix (see 2.3.2.1) and the corresponding density-sample matrix as input variables. The FD indices used in this study included: functional richness (FRic), functional evenness (FEve), functional divergence (FDiv) and the Rao's quadratic entropy (RaoQ) (Villéger et al., 2008). Each index reflects a different aspect of functional trait

space, and the way species are dispersed within this trait space (see Box 1 in Festjens et al., 2023). Apart from FRic, all indices take into account species abundance.

The potential of the community to influence ecosystem functioning such as nutrient cycling through sediment reworking can be estimated with the Bioturbation Potential Index, which incorporates species-specific bioturbation traits and structural attributes of the community (Solan et al., 2004). The bioturbation potential index (BP_c) was calculated for each sample according to Solan et al. (2004):

$$BP_c = \sum_{i=1}^n \sqrt{B_i/A_i} \times A_i \times M_i \times R_i$$

This metric is based on species-specific abundance (ind. m⁻²), biomass (g WW m⁻²) and a functional classification (i.e., mode scores) of sediment mixing-associated traits (M_i = mobility, R_i = sediment reworking) which were obtained from Queirós et al. (2013).

2.4. Statistical analyses

2.4.1. Univariate environmental and biological trends

The influence of distance to SPL edge (continuous) and OWF site (categorical) on the studied environmental and biological univariate response variables, was investigated using analysis of covariance (Ancova). End models were defined in a stepwise manner, starting from the most complex model including the interaction between distance and OWF site. If the end model only included the continuous predictor variable (distance), a simple linear regression was performed to investigate the distance effect on the considered variable. Prior to the model building, the assumption of linearity was tested together with the homogeneity of the regression slopes to assess whether the interaction term should be included in the most complex model. Assumptions of normality and homogeneity of variances (i.e., Shapiro and Levene tests) were assessed on the residuals of the end models. Results were visualized as regression plots with the predicted variation of points around the fitted regression line (standard error), based on the output of the final models.

2.4.2. Community composition

To investigate differences in terms of macrofaunal community composition, generalized linear models (GLMs) were constructed using the *manyglm* function (Wang et al., 2012). This function fits GLMs for each species in the dataset, using the resampling-based hypothesis to test the significance of the explanatory variables which included the term “OWF”, “Distance” and their interaction effect. Based on preliminary data exploration, a negative binomial distribution (log-link) was used to fit the models. Next, the significance of the explanatory variables was tested using the *anova.manyglm* function and species that contributed significantly to compositional differences were identified through the *p.uni* argument from the *mvabund* package (Niku et al., 2019; Wang et al., 2012).

2.4.3. Biological trait-based profile comparisons

From the species-trait score matrix (2.3.2.1), separate trait profiles were created for each OWF (C-Power and Belwind) and each distance (1 m, 7 m, 15 m and 25 m). Removal of absent species led to a profile dataset containing the compilation of fuzzy code values of the occurring species for each group (OWF site and distances). Next, the fuzzy code values were standardized, summed and transformed into percentages. Pearson Chi² tests were performed on the percentage values to compare trait categories between OWF sites, and between distances for both OWF site combined. When trait composition was found to differ significantly between distances, Chi² post-hoc tests were done, based on the standardized residuals with a critical values (CV) and corresponding *p*-values. Patterns in terms of significant biological traits were visualized as stacked bar plots, representing the percentual contribution of each

category to the total trait profile.

3. Results

3.1. Environmental patterns

Both granulometric properties (i.e., MGS and fine sand fraction) were significantly affected by the variables “Distance” and “OWF”, but not by their interaction (Table 2). MGS increased significantly with increasing distance from the SPL (estimate: 2.0 μm per m, Table 2), while an opposite pattern was found for the fine sand fraction (estimate: -0.26 % per m, Table 2) (Fig. 3). Sediments adjacent to D08 (MGS: 357 ± 6 μm, fine sand: 17 ± 1 %) were significantly finer compared to those adjacent to D05 (MGS: 383 ± 6 μm, fine sand: 11 ± 1 %). TOC and Chl-*a* contents were only significantly influenced by “OWF” and not by distance to the turbines (Table 3) (Supplementary Fig. 1). Both environmental variables showed higher average values adjacent to D05 within the C-Power OWF (TOC %: 0.044 ± 0.007 %, Chl-*a*: 0.244 ± 0.032 μg.g⁻¹ dry sediment) in comparison to adjacent to D08 in the Belwind OWF (TOC %: 0.024 ± 0.004 %, Chl-*a*: 0.099 ± 0.021 μg.g⁻¹ dry sediment).

3.2. Biological univariate patterns

3.2.1. Structural indices

Total macrofaunal abundance and species richness were comparable between D05 and D08, but both indices decreased significantly with increasing distance from the SPL (Fig. 4, Table 3) (TN: estimate = -22 ind. m⁻² per m, S: -0.49 species per m). In contrast, total macrofaunal biomass was comparable between D05 and D08 but was not affected by the distance relative to the turbines (Table 3). A more complex significant end model was found for the Shannon-Wiener diversity, showing that the decrease per meter distance away from the SPL was stronger at D05 compared to the D08 (Fig. 4, Table 3) (D05 estimate: -0.06 per m, D08 estimate: -0.02 per m).

3.2.2. Functional indices

The BPC levels decreased significantly with distance away from the SPL of both D08 and D05 (Fig. 5, Table 3), with each additional meter from the turbine resulting in an average decrease of 11 units in BPC. Species generally contributing most to overall BPC were the burrowing sea urchin *Echinocardium cordatum* and the polychaete *Nephtys cirrosa*, followed by the brittle star *Ophiura* juveniles, Nemertea (i.e., ribbon worms) and the amphipod *Urothoe brevicornis*. At closer distances (< 7 m), additional important contributing species to the BPC (≥ 4 % per species) included the starfish *Asterias rubens*, the tube polychaete *Lanice conchilega*, the brittle star *Ophiura albida* and the bivalve *Tellinmya ferruginosa*, while the amphipod *Bathyporeia elegans* and the polychaetes *Nephtys longosetosa* and *Ophelia borealis* were more important at distances ranging from 15 to 25 m from the turbines.

In terms of functional diversity indices, FRic decreased significantly

Table 2

Summary of the end models for the studied environmental parameters (response variables), showing the significance (*p*-value) of the included (i.e., Incl.) explanatory variables.

| Response variables | Distance | | OWF | | Distance*OWF | |
|---|----------|-----------------|-------|-----------------|--------------|-----------------|
| | Incl. | <i>p</i> -value | Incl. | <i>p</i> -value | Incl. | <i>p</i> -value |
| Median grain size (MGS, μm) | ✓ | 0.001 | ✓ | 0.045 | / | / |
| Fine sand fraction (< 250 μm, %) | ✓ | 0.002 | ✓ | 0.003 | / | / |
| Total organic carbon (TOC, %) | / | / | ✓ | 0.010 | / | / |
| Chlorophyll- <i>a</i> (Chl- <i>a</i> , μg/g dry sediment) | / | / | ✓ | 0.001 | / | / |

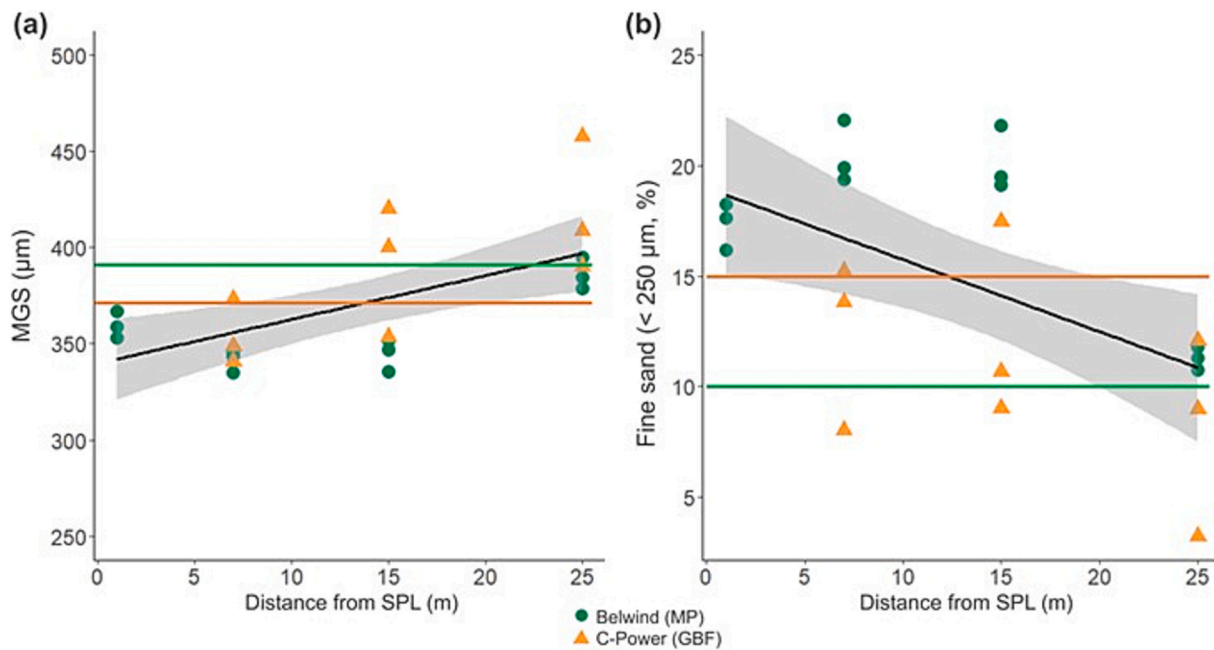


Fig. 3. Relationship between (a) median grain size (MGS, μm), (b) fine sand fraction ($< 250 \mu\text{m}$, %) and sampling distances (1 m–25 m) from the scour protection layer around the monopile (green circles, Belwind) and the gravity-based (orange triangle, C-Power) foundations. Grey shading represents standard errors. Horizontal lines represent the average of the corresponding parameters from the reference samples (2015–2019) at 240–570 m distance within Belwind (green) and C-Power (orange). (For interpretation of the references to colour in this figure legend, the reader is referred to the web version of this article.)

Table 3

Summary of end models for the studied biological parameters (response variables), showing the significance (p -value) of the included (i.e., Incl.) explanatory variables. * denote linear regression method to investigate the distance effect.

| Response variables | Distance | | OWF | | Distance*OWF | |
|---|----------|---------|-------|---------|--------------|---------|
| | Incl. | p-value | Incl. | p-value | Incl. | p-value |
| Total abundances (TN, ind. m^{-2})* | ✓ | < 0.001 | / | / | / | / |
| Total biomass (TB, g m^{-2})* | ✓ | 0.072 | / | / | / | / |
| Species richness (S, spp. sample^{-1})* | ✓ | < 0.001 | / | / | / | / |
| Shannon-Wiener diversity (H) | ✓ | 0.028 | ✓ | 0.017 | ✓ | 0.001 |
| Bioturbation potential (BPC)* | ✓ | 0.012 | / | / | / | / |
| Functional richness (Fric)* | ✓ | 0.001 | / | / | / | / |
| Functional evenness (FEve) | / | / | ✓ | 0.017 | / | / |
| Functional divergence (FDiv)* | ✓ | 0.065 | / | / | / | / |
| Rao's quadratic entropy (RaoQ) | ✓ | < 0.001 | ✓ | 0.002 | ✓ | <0.001 |

with 17 units per m away from D05 and D08 (Fig. 5, Table 3) whereas FEve was not affected by the distance from the SPL, but was significantly higher adjacent to D05 in C-Power (average FEve: 0.70 ± 0.09) compared to D08 in Belwind (average FEve: 0.60 ± 0.07) (Table 3) (Supplementary Fig. 2). FDiv values were similar adjacent to D08 and D05 and were not significantly predicted by distance away from the SPL (Table 3). Finally, the significant end model for RaoQ showed that the decrease per meter distance away from the SPL was stronger at D05 compared to the D08 (Fig. 5, Table 3) (D05 estimate: -1.9 per m, D08 estimate: -0.18 per m).

3.3. Macrobenthic community composition

Multivariate GLM analysis showed that “Distance” ($p = 0.001$, deviance = 156.15), “OWF” ($p = 0.001$, deviance = 204.61), and their interaction “Distance \times OWF” ($p = 0.006$, deviance = 56.24) significantly influenced macrobenthic community composition. Bivalvia juveniles were significantly associated with “Distance,” occurring exclusively in samples taken 1 m from the SPL. Three species (i.e., *Lanice conchilega*, *Ophiura* juveniles and *Bathyporeia elegans*) contributed significantly to the differences in composition between D05 and D08 (parameter “OWF”, Supplementary Table 3). The tube-building polychaete *Lanice conchilega* was exclusively found at 7 m distance away from the D05 SPL, while the other two species were more abundant adjacent to D08 in Belwind (Supplementary Tables 4, 5). *Ophiura* juveniles also contributed significantly to the interaction term, with highest abundances between 1 and 7 m and higher occurrences near the monopile compared to the GBF.

3.4. Biological trait profile comparisons

Modality compositions did not differ between OWF but distance-dependent differences were found for three biological traits, i.e. the response traits “mobility” ($p = 0.001$) and “sediment position” ($p = 0.005$), and the effect trait “bioturbation” ($p < 0.001$), while the effect trait “feeding mode” was borderline significant ($p = 0.054$). The other biological trait profiles were similar across distances ($p > 0.05$). In general, mobility profiles were composed by all four categories, with highest percentages for burrowers and crawlers. In terms of sediment position, trait profiles were mainly represented by surface dwellers, infauna (0–5 cm) and deeper infauna (6–10 cm). Bioturbation trait profiles were characterized by highest percentages of diffusive mixing and surface depositors at each distance, and the absence of downward conveyors. All feeding modes, except for parasites, were represented across distances, with highest percentages for surface feeders, followed by suspension feeders, predators and subsurface deposit feeders (Fig. 6).

Post-hoc testing further highlighted that spatial differences between biological trait profiles existed between 25 m and the other sampling

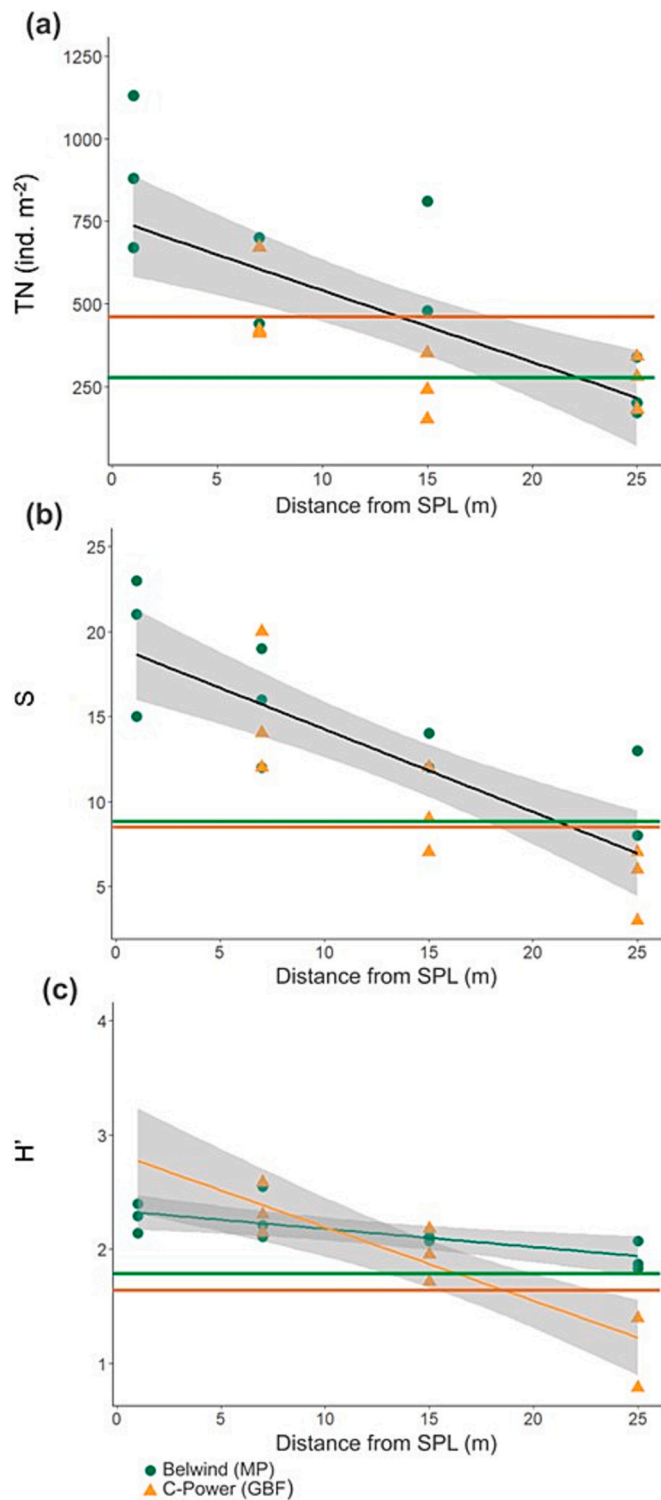


Fig. 4. Relationship between sampling distance from the scour protection layer (1 m–25 m) and structural biological indices (a) total abundance (TN, ind. m⁻²), (b) species richness (S), and (c) Shannon-Wiener diversity (H') around the D08 monopile (Belwind) and the D05 gravity-based (C-Power) foundations. Grey shading represents standard errors. Horizontal lines represent average values of the corresponding parameters for the reference samples (2015–2019) at 240–570 m distance within Belwind (green) and C-Power (orange). (For interpretation of the references to colour in this figure legend, the reader is referred to the web version of this article.)

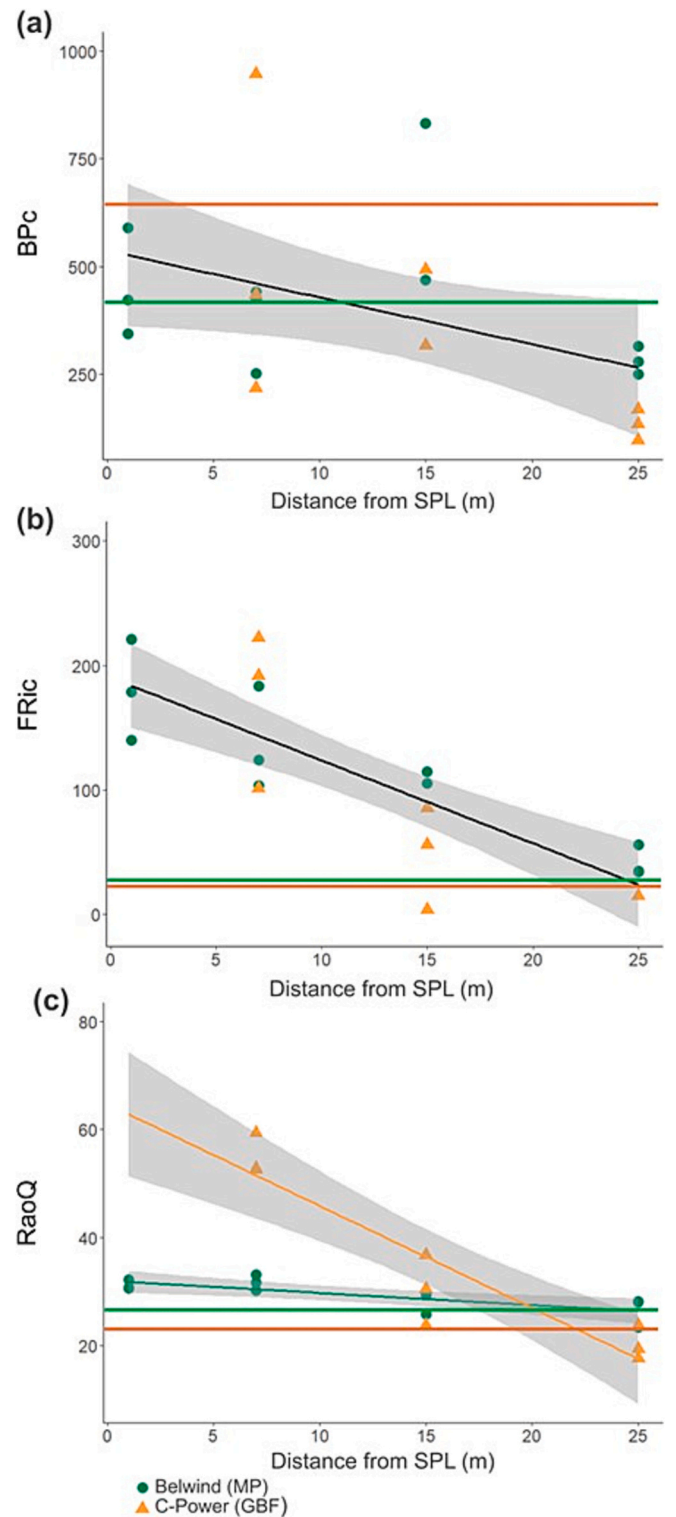


Fig. 5. Relationship between sampling distance from the scour protection layer (1 m–25 m) and functional biological indices (a) bioturbation potential (BPc), (b) functional richness (Fric), and (c) Rao's quadratic entropy (RaoQ) around the D08 monopile (Belwind) and the D05 gravity-based (C-Power) foundations. Grey shading represents standard errors. Horizontal lines represent average values of the corresponding parameters for the reference samples (2015–2019) at 240–570 m distance within Belwind (green) and C-Power (orange). (For interpretation of the references to colour in this figure legend, the reader is referred to the web version of this article.)

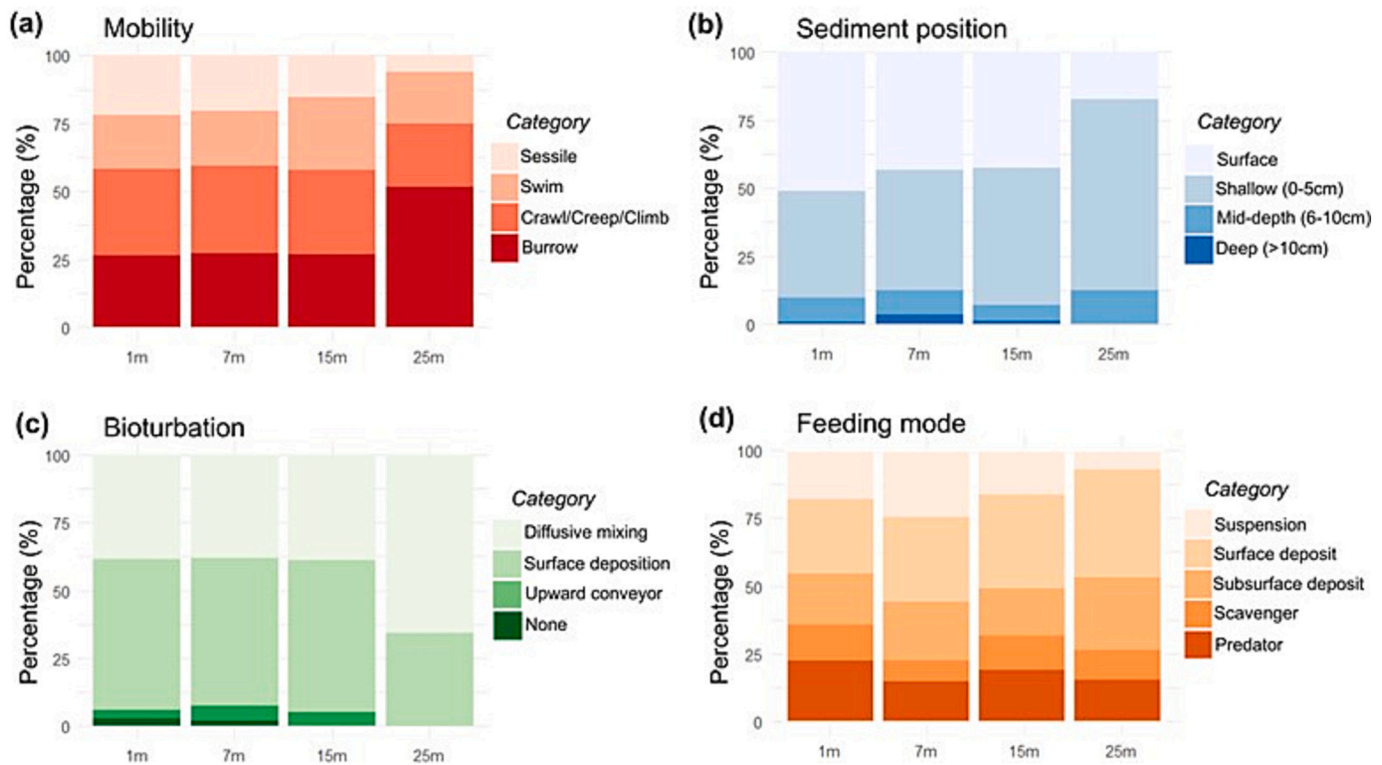


Fig. 6. Stacked bar plots with percental contributions of each category to the total trait profile per distance (1 m–25 m) for the four biological traits (a) mobility, (b) sediment position, (c) bioturbation and (d) feeding mode around the D08 monopile (Belwind) and D05 gravity-based (C-Power) foundations.

distances. At 25 m, the percentage of burrowers and surface dwellers was significantly lower than at all other distances (burrower CV: -2.95 , residual value: -3.16 , $p = 0.03$; surface dwellers CV: -2.95 , residual value: 4.58 , $p < 0.001$), while shallow living infauna (0-5 cm) showed higher percentages at this distance (CV: -2.96 , residual value: 4.45 , $p < 0.001$) (Fig. 6). Relative abundances of diffusive mixers were significantly higher at 25 m from the SPL (CV: -2.95 , residual value: 4.71 , $p < 0.001$), while surface depositors was lower compared to closer distances (CV: -2.95 , residual value: -3.62 , $p = 0.005$). Suspension feeders were less dominant at 25 m, but the corresponding post-hoc test was not significant ($p = 0.063$).

4. Discussion

Our study confirmed that AR effects occur in soft-sediment habitats in the residual current direction from the SPL of offshore cylindrical turbine foundations, but that their spatial extent is limited and the magnitude decreases with distance from the turbine foundation. At 25 m from the SPL, environmental and biological conditions were comparable with reference samples located further away (240-570 m). Within the 15 m range of the SPL, biological responses included higher macrofaunal abundances and diversity, both at the structural and functional level. In contrast to some dissimilarities in structural community composition, biological trait profiles were similar in sediments around gravity-based and monopile foundations, confirming the selection of specific traits at the investigated sites. Moreover, the biological trait analysis revealed a clear spatial distinction in terms of sediment position, mobility, feeding and bioturbation modalities between communities located at closer ranges (≤ 15 m) and those at 25 m from the SPL. Interestingly, the response traits “mobility” and “sediment position” were observed to align with the change along the sediment gradient within the benthic AR zone, whereas the spatial patterns in the effect trait “bioturbation” merely reflected a segregation between the sediment in and outside the AR. Likewise, Bolam et al. (2023) found in an extensive study of UK shelf

sediments that response traits were found to be better predicted from environmental variables than effect trait expressions, suggesting that response traits are more mechanistically linked to environmental conditions, like sediment type, and are thus more inherently tied to how organisms react to environmental gradients.” These spatial patterns in response and effect traits therefore shed light into physical and biological community assembly rules that shape the AR effect on the soft-sediment (i.e. sediment fining, organic enrichment and biofouling drop-offs, see below), as well as its potential functional implications.

Sediments in the wake of both turbine foundation types became progressively finer closer to the SPL. Hydrodynamic obstruction by closed cylindrical structures induce swirling vortices that enhance sediment resuspension downstream of the foundation, resulting in turbid wakes and retention areas where finer-grained particles deposit (Christiansen et al., 2023; Floeter et al., 2017), explaining the observed sediment fining gradient away from the SPL in this study. This gradient was associated with higher macrobenthic abundance and species richness closer to the SPL. Our BTA revealed that this response is predominantly driven by increased species occurrences and population abundances of surface-dwelling sessile and crawling fauna, whereas deeper living burrowers that can migrate away from unfavourable conditions (strong currents) dominated in the coarser sediments at 25 m. This shift in mobility and sediment position traits correspond to Godefroo et al. (2023) who described a positive association between fine sand fractions and crawlers and sessile species, and a negative relationship between median grain size and burrowing species in offshore sediments in the BPNS. Yet, hydrodynamically-induced grain size fining that facilitates surface-dwelling macrobenthos, including habitat-forming species (see further), can be identified as an important governing mechanism of the benthic AR effect. The similarities with the results of Coates et al. (2014) from the same GBF a decade ago demonstrate that such sediment fining is a persistent AR mechanism. However, our study also shows that small-scale variability in local fining can exist within the area of the AR footprint, especially when the turbine

foundation is positioned at the slope of the sandbank and therefore prone to the higher erosion of sands from the SPL filter layer. Despite the vastly larger surface area of the D05 turbine GBF and its surrounding SPL (Fig. 1), the stronger hydrodynamics associated with that slope habitat may also have obliterated the spatial extension of the local AR footprint by inhibiting the further expansion of habitat-forming species such as the tube-building polychaetes *Lanice conchilega* and *Owenia fusiformis* that require more benign conditions for recruitment (see e.g. Callaway, 2003 and references therein). Both species solely occurred at the closest sampling location in the C-Power OWF with densities up to 140 and 70 ind.m⁻², respectively (Supplementary Table 4). Tube-building polychaetes can locally increase biodiversity through ecosystem engineering activities (Rabaut et al., 2009; Rabaut et al., 2007), and their presence therefore likely contributed to the particularly high RaoQ index close to the SPL of D05. One exception to the sediment fining gradient is the locally coarser grain size at 1 m from the SPL around the monopile. Mobile sand covers the filter layer of the SPL and sediment cores taken very close to the SPL most likely contain traces of this coarser filter layer.

In addition to physical processes, our results also show that interaction with the epifaunal communities growing on the AR play a role in shaping its footprint on the adjacent soft-sediment. Firstly, epifaunal species or byproducts (e.g., shell litter) can fall off from the structures owing to their weight and/or hydrological forcing (Degraer et al., 2020; Hutchison et al., 2020; Lefaible et al., 2023). For example, in our study, the biofouling suspension feeding species, *Jassa herdmani*, did show higher abundances (up to 80 ind.m⁻²; Supplementary Tables 4, 5) in the soft-sediment closest to the cylindrical turbines. These amphipods entrap sediment and organic matter to build their tubes, thereby creating microhabitats for species such as the polychaete *Phyllodoce mucosa* (Zintzen et al., 2008; Zupan et al., 2023), a species that was also exclusively observed in the sediments up to 15 m away from the turbines (Supplementary Tables 4, 5). In addition to other habitat-forming species, like *L. conchilega* and *O. fusiformis*, the presence of dropped biofouling species like *Jassa herdmani* can thus also contribute to the more diverse infaunal communities compared to sediments outside of the AR footprint. Secondly, experiments and modeling demonstrate that deposition of faecal pellets (i.e. biodeposition) from suspension-feeding biofoulers is likely an important source of organic enrichment for the surrounding seabed (Ivanov et al., 2021; De Borger et al., 2021). However, observational and quantitative evidence for this organic enrichment hypothesis remains scant, as is the case in the present study which did not find a significant distance effect on sediment TOC and chl-*a* content. This can be explained by several reasons. Firstly, biodeposits may be patchily distributed. Hence, biodeposits and aggregated species distributions may have been missed in this study due to undersampling, i.e. three replicates per location. Secondly, aerobic degradation of organic-rich biodeposits occurs fast in permeable sediments (Huettel et al., 2014), thereby inhibiting the accumulation of organic matter. Thirdly, because the Southern Bight of the North Sea is characterized by a strong seasonality in terms of phytoplankton production (Fettweis et al., 2022) and subsequent biodeposition at the seabed (Provoost et al., 2013), the enrichment from phytodetritus in April–May would likely have disappeared by Autumn when sampling took place. Indeed, whereas the sediments <15 m of the SPL are finer compared to the reference conditions, they are still considered permeable (based on actual sediment permeability measurements; De Borger et al. unpublished results) and subject to regular flushing with oxygen-rich water. Actually, the exclusive occurrence of upward conveyers and the increased dominance of surface depositors in the area of the AR footprint, could have facilitated such organic matter mineralization (Kristensen et al., 2012). Nevertheless, such temporal additional food input via the water column can support the more diverse and abundant macrobenthos community in the AR footprint area.

Through the use of BTA, our study provides valuable quantitative information on how AR-induced response trait effects, i.e. shift towards

more surface-associated benthos, can influence trophic energy transfer, organic matter capture and mineralization via accompanied changes in effect traits. The AR benthic footprint was characterized by clear increase in macrofaunal structural and functional diversity, which constitutes an enhanced and more diversified prey availability for higher trophic levels. Indeed, the role of artificial reefs to act as a nursery for the larvae of decapod species, including those residing in the AR, as hypothesized by Hooper and Austen (2014), seems supported through the observed increased abundances of predatory decapod juveniles most adjacent to the SPL (83 ± 9 ind.m⁻²; Supplementary Tables 4, 5) where the sessile and other surface-dwelling macrofauna could represent favourable prey items. In general the shift towards a macrobenthos community with a more even representation of different feeding modes, including suspension feeders, hints at efficient energy cycling and tight connection with the epifaunal community on the SPL and turbine. Further, the shift to more surface depositors, and in general the occurrence of more diverse sediment reworking modes, highlights the increasing role of biological sediment reworking activity in overall nutrient recycling within the area of the AR benthic footprint. Despite the great effort in mechanistically linking specific trait modalities with ecosystem function in lab-based and in situ experimental work (e.g. O'Meara et al., 2020; Wrede et al., 2019), understanding how such effect trait responses relate to true changes in nutrient cycling and thus represent good surrogates for ecological functioning remains to be investigated, in particular given the potential that trait expressions can change depending on species interactions and the local abiotic sediment environment (Cassidy et al., 2020; Van Colen et al., 2013).

5. Conclusion

Our study confirms that cylindrical turbine foundations and their SPL affect surrounding soft-sediment habitats. In comparison to documented spatial effects for fish and macrocrustaceans (Glarou et al., 2020 and references therein), the spatial extent of the observed AR effects, however, remains restricted to a relatively small footprint after 10–13 years. The spatially restricted soft-sediment AR footprint in the wake of the turbines explains why no ecological changes were detected by Lefaible et al. (2023) at 37.5 m from the SPL of monopiles in the same OWF. However, the spatial dynamics of the footprint may well depend on the local hydrodynamics (i.e. in versus outside of the wake) and differ between offshore sandbank systems. For example habitats with finer sediments than the permeable sediments investigated here, may accumulate organic matter over longer time scales with cascading effects on the local biodiversity. Finally, the OWF site-dependent distance effect on the (functional) diversity found in this study also confirms that the local conditions, e.g. position on the sandbank (Cheng et al., 2021) can shape the AR effect. Nevertheless, biological responses were consistent with studies around different turbine foundation types such as jackets or other marine industries (e.g., offshore bivalve aquaculture, oil and gas platforms) (Keeley et al., 2013; Mascorda Cabre et al., 2021; Sun et al., 2021), indicating that the underlying mechanisms supported by our biological trait approach are universal.

CRedit authorship contribution statement

Nene Lefaible: Writing – review & editing, Writing – original draft, Visualization, Investigation, Formal analysis, Data curation, Conceptualization. **Carl Van Colen:** Writing – review & editing, Validation, Supervision, Investigation. **Christelle Jamar:** Writing – review & editing, Investigation, Formal analysis, Data curation. **Jan Vanaverbeke:** Writing – review & editing, Funding acquisition, Conceptualization. **Tom Moens:** Writing – review & editing, Project administration, Funding acquisition. **Sven Van Haelst:** Resources, Methodology. **Alain Norro:** Writing – review & editing, Resources, Methodology. **Steven Degraer:** Writing – review & editing, Funding acquisition. **Ulrike Braeckman:** Writing – review & editing, Validation,

Supervision, Resources, Project administration, Methodology, Investigation, Funding acquisition, Conceptualization.

Declaration of competing interest

The authors declare that they have no known competing financial interests or personal relationships that could have appeared to influence the work reported in this paper.

Acknowledgments

Field work could not have been completed without the help and smooth operation provided by the officers and crew of the RV Belgica, owned by the Belgian Ministry of Science Policy and coordinated by RBINS-OD Nature, and the RV Simon Stevin, property of the Flemish government and coordinated by VLIZ. The sampling was performed by the Belgian Occupational Scientific Diving team, coordinated by Dr. Alain Norro (RBINS) and Sven Van Haelst (VLIZ), which is part of the contribution of the Institute of Natural Sciences to EMBRC Belgium. We thank the operators of the C-Power and BelWind OWFs for their willing cooperation throughout the monitoring, in fulfilment of the monitoring requirements of their environmental permit. We are grateful to Bruno Vlaeminck for pigment analysis and to Bart Beuselinck for granulometry and TOC measurements. A special thanks to Felien Festjens for the help with the calculation of the functional diversity indices and Mirta Zupan for the explanation of the multivariate analysis (manyglm). This research and sample processing was carried out with infrastructure funded by EMBRC Belgium - FWO international research infrastructure I001621N. This work was also supported by the Belgian Science Policy Offices (BELSPO), the OUTFLOW project and the WinMon.BE monitoring program. This study contributes to the BELSPO FED-tWIN METRIC project: Marine Ecosystem Responses In a multiple pressures Context.

Data availability

Data will be made available on request.

References

- Baeye, M., Fettweis, M., 2015. In situ observations of suspended particulate matter plumes at an offshore wind farm, Southern North Sea. *Geo-Mar. Lett.* 35 (4), 247–255. <https://doi.org/10.1007/s00367-015-0404-8>.
- Bolam, S.G., McIlwaine, P.S.O., Garcia, C., 2016. Application of biological traits to further our understanding of the impacts of dredged material disposal on benthic assemblages. *Mar. Pollut. Bull.* 105 (1), 180–192. <https://doi.org/10.1016/j.marpolbul.2016.02.031>.
- Bolam, S.G., Cooper, K., Downie, A.-L., 2023. Mapping marine benthic biological traits to facilitate future sustainable development. *Ecol. Appl.* 33 (7), e2905. <https://doi.org/10.1002/eap.2905>.
- Boutin, K., Gaudron, S.M., Denis, J., Lasram, Ben Rais, F., 2023. Potential marine benthic colonisers of offshore wind farms in the English channel: a functional trait-based approach. *Mar. Environ. Res.* 190 (June). <https://doi.org/10.1016/j.marenvres.2023.106061>.
- Brandao, I.L.S., van der Molen, J., van der Wal, D., 2023. Effects of offshore wind farms on suspended particulate matter derived from satellite remote sensing. *Sci. Total Environ.* 866 (August 2022), 161114. <https://doi.org/10.1016/j.scitotenv.2022.161114>.
- Breine, N.T., De Backer, A., Van Colen, C., Moens, T., Hostens, K., Van Hoey, G., 2018. Structural and functional diversity of soft-bottom macrobenthic communities in the Southern North Sea. *Estuar. Coast. Shelf Sci.* 214 (April), 173–184. <https://doi.org/10.1016/j.ecss.2018.09.012>.
- Bremner, J., Rogers, S.I., Frid, C.L.J., 2006. Methods for describing ecological functioning of marine benthic assemblages using biological traits analysis (BTA). *Ecol. Indic.* 6, 609–622. <https://doi.org/10.1016/j.ecolind.2005.08.026>.
- Buyse, J., Reubens, J., Hostens, K., Degraer, S., Goossens, J., De Backer, A., 2023. European plaice movements show evidence of high residency, site fidelity, and feeding around hard substrates within an offshore wind farm. *ICES J. Mar. Sci.* 1–13. <https://doi.org/10.1093/icesjms/fsad179>. July.
- Callaway, R., 2003. Juveniles stick to adults: recruitment of the tube-dwelling polychaete *Lanice conchilega* (Pallas, 1766). *Hydrobiologia* 503, 121–130. <https://doi.org/10.1023/B:HYDR.0000008494.20908.87>.
- Cassidy, L.C., Godbold, J.A., Hale, R., Solan, M., 2020. Species identity, density and environmental history alter trait expression in brittlestars and change ecosystem functioning. *Proc. R. Soc. B Biol. Sci.* 287 (1929), 20202143. <https://doi.org/10.1098/rspb.2020.2143>.
- Chen, H.H., Yang, R.Y., Hwung, H.H., 2014. Study of hard and soft countermeasures for scour protection of the jacket-type offshore wind turbine foundation. *J. Mar. Sci. Eng. 2* (3), 551–567. <https://doi.org/10.3390/jmse2030551>.
- Cheng, C.H., Ysebaert, T., Borsje, B.W., Soetaert, K., Beauchard, O., O'Flynn, S., 2021. Small-scale macrobenthic community structure along asymmetrical sand waves in an underwater seascape. *Mar. Ecol.* 42 (2), e12657. <https://doi.org/10.1111/maec.12657>.
- Christiansen, N., Carpenter, J.R., Daewel, U., Suzuki, N., Schrum, C., 2023. The large-scale impact of anthropogenic mixing by offshore wind turbine foundations in the shallow North Sea. *Front. Mar. Sci.* 10 (May), 1–17. <https://doi.org/10.3389/fmars.2023.1178330>.
- Coates, D.A., Deschutter, Y., Vincx, M., Vanaverbeke, J., 2014. Enrichment and shifts in macrobenthic assemblages in an offshore wind farm area in the Belgian part of the North Sea. *Mar. Environ. Res.* 95, 1–12. <https://doi.org/10.1016/j.marenvres.2013.12.008>.
- Coolen, J.W.P., Vanaverbeke, J., Dannheim, J., Garcia, C., Birchenough, S.N.R., Krone, R., Beermann, J., 2022. Generalized changes of benthic communities after construction of wind farms in the southern North Sea. *J. Environ. Manag.* 315 (May), 115173. <https://doi.org/10.1016/j.jenvman.2022.115173>.
- Dannheim, J., Bergström, L., Birchenough, S.N.R., Brzana, R., Boon, A.R., Coolen, J.W.P., Dauvin, J.C., De Mesel, I., Derweduwien, J., Gill, A.B., Hutchison, Z.L., Jackson, A.C., Janas, U., Martin, G., Raoux, A., Reubens, J., Rostin, L., Vanaverbeke, J., Wilding, T. A., Degraer, S., 2020. Benthic effects of offshore renewables: identification of knowledge gaps and urgently needed research. *ICES J. Mar. Sci.* 77 (3), 1092–1108. <https://doi.org/10.1093/icesjms/fsz018>.
- De Borger, E., Ivanov, E., Capet, A., Braeckman, U., Vanaverbeke, J., Grégoire, M., Soetaert, K., 2021. Offshore windfarm footprint of sediment organic matter mineralization processes. *Front. Mar. Sci.* 8 (June), 1–16. <https://doi.org/10.3389/fmars.2021.632243>.
- De Mesel, I., Kerckhof, F., Norro, A., Rumes, B., Degraer, S., 2015. Succession and seasonal dynamics of the epifauna community on offshore wind farm foundations and their role as stepping stones for non-indigenous species. *Hydrobiologia* 756, 37–50. <https://doi.org/10.1007/s10750-014-2157-1>.
- deCastro, M., Salvador, S., Gómez-Gesteira, M., Costoya, X., Carvalho, D., Sanz-Larruga, F.J., Gimeno, L., 2019. Europe, China and the United States: three different approaches to the development of offshore wind energy. *Renew. Sust. Energy Rev.* 109 (February), 55–70. <https://doi.org/10.1016/j.rser.2019.04.025>.
- Degraer, S., Carey, D.A., Coolen, J.W.P., Hutchison, Z.L., Kerckhof, F., Rumes, B., Vanaverbeke, J., 2020. Offshore wind farm artificial reefs affect ecosystem structure and functioning: a synthesis. *Oceanography* 33 (4), 48–57. <https://doi.org/10.5670/oceanog.2020.405>.
- Féral, Jean-Pierre, Norro, Alain, 2023. Specific initial training standards are needed to dive for science in Europe, occupational vs. citizen science diving. *Front. Mar. Sci.* <https://doi.org/10.3389/fmars.2023.1134494>.
- Festjens, F., Buyse, J., De Backer, A., Hostens, K., Lefaible, N., Vanaverbeke, J., Van Hoey, G., 2023. Functional trait responses to different anthropogenic pressures. *Ecol. Indic.* 146 (January), 109854. <https://doi.org/10.1016/j.ecolind.2022.109854>.
- Fettweis, M., Schartau, M., Desmit, X., Lee, B.J., Tereleer, N., Van der Zande, D., Parmentier, K., Riethmüller, R., 2022. Organic matter composition of biomineral flocs and its influence on suspended particulate matter dynamics along a nearshore to offshore transect. *J. Geophys. Res. Biogeosci.* 127 (1), 1–34. <https://doi.org/10.1029/2021JG006332>.
- Floeter, J., van Beusekom, J.E.E., Auch, D., Callies, U., Carpenter, J., Dudeck, T., Eberle, S., Eckhardt, A., Gloe, D., Hänselein, K., Hufnagl, M., Janßen, S., Lenhart, H., Möller, K.O., North, R.P., Pohlmann, T., Riethmüller, R., Schulz, S., Spreizenbarth, S., Möllmann, C., 2017. Pelagic effects of offshore wind farm foundations in the stratified North Sea. *Prog. Oceanogr.* 156, 154–173. <https://doi.org/10.1016/j.pocean.2017.07.003>.
- Galparsoro, I., Menchaca, I., Garmendia, J.M., Borja, Á., Maldonado, A.D., Iglesias, G., Bald, J., 2022. Reviewing the ecological impacts of offshore wind farms. *NPJ Ocean Sustain.* 1 (1), 1–8. <https://doi.org/10.1038/s44183-022-00003-5>.
- Glarou, M., Zrust, M., Svendsen, J.C., 2020. Using artificial-reef knowledge to enhance the ecological function of offshore wind turbine foundations: implications for fish abundance and diversity. *J. Mar. Sci. Eng.* 8 (5). <https://doi.org/10.3390/JMSE8050332>.
- Goedefroo, N., Braeckman, U., Hostens, K., Vanaverbeke, J., Moens, T., De Backer, A., 2023. Understanding the impact of sand extraction on benthic ecosystem functioning: a combination of functional indices and biological trait analysis. *Front. Mar. Sci.* 10 (October), 1–15. <https://doi.org/10.3389/fmars.2023.1268999>.
- Gutow, L., Daniels, M., Mielck, F., Zielinski, O., 2014. Artificial hard substrates in the German Bight—Faunal colonization and implications for offshore wind farm design. In: *Benthic Habitats and the Effects of Offshore Structures. Proceedings of the 3rd International Workshop, Wilhelmshaven, Germany. Institute of Marine Research, Wilhelmshaven.*
- Hooper, T., Austen, M., 2014. The co-location of offshore windfarms and decapod fisheries in the UK: constraints and opportunities. *Mar. Policy* 43, 295–300. <https://doi.org/10.1016/j.marpol.2013.06.011>.
- Huettel, M., Berg, P., Kostka, J.E., 2014. Benthic exchange and biogeochemical cycling in permeable sediments. *Annu. Rev. Mar. Sci.* 6, 23–51. <https://doi.org/10.1146/annurev-marine-051413-012706>.
- Hutchison, Z.L., Bartley, M.L., Degraer, S., English, P., Khan, A., Livermore, J., Rumes, B., King, J.W., 2020. Offshore wind energy and benthic habitat changes lessons from block island wind farm. *Oceanography* 33 (4), 58–69. <https://doi.org/10.5670/oceanog.2020.406>.

- Ivanov, E., Capet, A., De Borger, E., Degraer, S., Delhez, E.J.M., Soetaert, K., Vanaverbeke, J., Grégoire, M., 2021. Offshore wind farm footprint on organic and mineral particle flux to the bottom. *Front. Mar. Sci.* 8, 631799. <https://doi.org/10.3389/fmars.2021.631799>.
- Jak, R., Glorius, S.T., 2017. *Macrobenthos in Offshore Wind Farms: A Review of Research, Results and Relevance for Future Developments*. Wageningen Marine Research report C043/17. Wageningen University & Research, Den Helder, the Netherlands. <https://doi.org/10.18174/415357>.
- Jammar, C., Reynés-Cardona, A., Vanaverbeke, J., Lefaible, N., Moens, T., Degraer, S., Braeckman, U., 2025. Decadal trends in macrobenthic communities in offshore wind farms: disentangling turbine and climate effects. *J. Sea Res.* 203, 102557.
- Keeley, N.B., Forrest, B.M., Macleod, C.K., 2013. Novel observations of benthic enrichment in contrasting flow regimes with implications for marine farm monitoring and management. *Mar. Pollut. Bull.* 66 (1–2), 105–116. <https://doi.org/10.1016/j.marpolbul.2012.10.024>.
- Kerckhof, F., Rumes, B., Norro, A., Jacques, T.G., Degraer, S., 2010. Seasonal variation and vertical zonation of the marine biofouling on a concrete offshore windmill foundation on the Thornton Bank (southern North Sea). In: Degraer, S., Brabant, R., Rumes, B. (Eds.), *Offshore Wind Farms in the Belgian Part of the North Sea: Early Environmental Impact Assessment and Spatio-Temporal Variability*. Royal Belgian Institute of Natural Sciences, Brussels, pp. 53–68.
- Kingma, E.M., ter Hofstede, R., Kardinaal, E., Bakker, R., Bittner, O., van der Weide, B., Coolen, J.W.P., 2024. Guardians of the seabed: nature-inclusive design of scour protection in offshore wind farms enhances benthic diversity. *J. Sea Res.* 199 (April), 102502. <https://doi.org/10.1016/j.seares.2024.102502>.
- Kristensen, E., Penha-Lopes, G., Delefosse, M., Valdemarsen, T., Quintana, C.O., Banta, G. T., 2012. What is bioturbation? The need for a precise definition for fauna in aquatic sciences. *Mar. Ecol. Prog. Ser.* 446, 285–302. <https://doi.org/10.3354/meps09506>.
- Lacroix, G., Ruddick, K., Ozer, J., Lancelot, C., 2004. Modelling the impact of the Scheldt and Rhine/Meuse plumes on the salinity distribution in Belgian waters (southern North Sea). *J. Sea Res.* 52 (3), 149–163. <https://doi.org/10.1016/j.seares.2004.01.003>.
- Laliberté, E., Legendre, P., 2010. A distance-based framework for measuring functional diversity from multiple traits. *Ecology* 91 (1), 299–305. <https://doi.org/10.1890/08-2244.1>.
- Lefaible, N., Braeckman, U., Degraer, S., Vanaverbeke, J., Moens, T., 2023. A wind of change for soft-sediment infauna within operational offshore windfarms. *Mar. Environ. Res.* 188 (April), 106009. <https://doi.org/10.1016/j.marenvres.2023.106009>.
- Mascorda Cabre, L., Hosegood, P., Attrill, M.J., Bridger, D., Sheehan, E.V., 2021. Offshore longline mussel farms: a review of oceanographic and ecological interactions to inform future research needs, policy and management. *Rev. Aquac.* 13 (4), 1864–1887. <https://doi.org/10.1111/raq.12549>.
- Mavraki, N., De Mesel, I., Degraer, S., Moens, T., Vanaverbeke, J., 2020. Resource niches of co-occurring invertebrate species at an offshore wind turbine indicate a substantial degree of trophic plasticity. *Front. Mar. Sci.* 7 (June), 1–17. <https://doi.org/10.3389/fmars.2020.00379>.
- Mavraki, N., Coolen, J.W.P., Kapasakali, D.A., Degraer, S., Vanaverbeke, J., Beermann, J., 2022. Small suspension-feeding amphipods play a pivotal role in carbon dynamics around offshore man-made structures. *Mar. Environ. Res.* 178 (October 2021), 105664. <https://doi.org/10.1016/j.marenvres.2022.105664>.
- Miles, J., Martin, T., Goddard, L., 2017. Current and wave effects around windfarm monopile foundations. *Coast. Eng.* 121, 167–178. <https://doi.org/10.1016/j.coastaleng.2017.01.003>.
- Niku, J., Hui, F.K.C., Taskinen, S., Warton, D.I., 2019. Gllvm: fast analysis of multivariate abundance data with generalized linear latent variable models in R. *Methods Ecol. Evol.* 10 (12), 2173–2182. <https://doi.org/10.1111/2041-210X.13303>.
- O'Meara, T.A., Hewitt, J.E., Thrush, S.F., Douglas, E.J., Lohrer, A.M., 2020. Denitrification and the role of macrofauna across estuarine gradients in nutrient and sediment loading. *Estuar. Coasts* 43 (6), 1394–1405. <https://doi.org/10.1007/s12237-020-00728-x>.
- Pardo, J.C.F., Aune, M., Harman, C., Walday, M., Skjellum, S.F., 2025. A synthesis review of nature positive approaches and coexistence in the offshore wind industry. *ICES J. Mar. Sci.* 82 (4), 1–17. <https://doi.org/10.1093/icesjms/fsad191>.
- Provoost, P., Braeckman, U., Van Gansbeke, D., Moodley, L., Soetaert, K., Middelburg, J. J., Vanaverbeke, J., 2013. Modelling benthic oxygen consumption and benthic–pelagic coupling at a shallow station in the southern North Sea. *Estuar. Coast. Shelf Sci.* 120, 1–11. <https://doi.org/10.1016/j.ecss.2013.01.008>.
- Prusina, I., Hermans, A., Bos, O.G., Klinge, M., 2020. *Nature-Inclusive Design: a catalogue for offshore wind infrastructure* the Ministry of Agriculture. Nat. Food Qual. <https://doi.org/10.13140/RG.2.2.10942.02882>. Final version. March.
- Queirós, A.M., Birchenough, S.N., Bremner, J., Godbold, J.A., Parker, R.E., Romero-Ramirez, A., Widdicombe, S., 2013. A bioturbation classification of European marine infaunal invertebrates. *Ecol. Evol.* 3 (11), 3958–3985.
- Rabaut, M., 2007. A bio-engineered soft-bottom environment: the impact of *Lanice conchilega* on the benthic species-specific densities and community structure. *Estuar. Coast. Shelf Sci.* 75 (4), 525–536.
- Rabaut, M., Du Four, I., Nakas, G., Van Lancker, V., Degraer, S., Vincx, M., 2009. Ecosystem engineers stabilize sand bank systems: *Owenia fusiformis* aggregations as ecologically important microhabitat. In: Rabaut, M. (Ed.), *Bedforms as Benthic Habitats: Living on the Edge*. VLIZ Special Publication 43, Flanders Marine Institute (VLIZ), Ostende, Belgium, pp. 101–116.
- Rendle, E.J., Hunt, E.L., Bicknell, A.W.J., 2023. A three-step approach for co-locating nature-based solutions within offshore wind farms. *Front. Ecol. Evol.* 11 (June), 1–19. <https://doi.org/10.3389/fevo.2023.690382>.
- Solan, M., Cardinale, B.J., Downing, A.L., Engelhardt, K.A.M., Ruesink, J.L., Srivastava, D.S., 2004. Extinction and ecosystem function in the marine benthos. *Science* 306 (5699), 1177–1180. <https://doi.org/10.1126/science.1103960>.
- Sun, X., Dong, J., Hu, C., Zhang, Y., Chen, Y., Zhang, X., 2021. Use of macrofaunal assemblage indices and biological trait analysis to assess the ecological impacts of coastal bivalve aquaculture. *Ecol. Indic.* 127, 107713. <https://doi.org/10.1016/j.ecolind.2021.107713>.
- ter Hofstede, R., Driessen, F.M.F., Elzinga, P.J., Van Koningsveld, M., Schutter, M., 2022. Offshore wind farms contribute to epibenthic biodiversity in the North Sea. *J. Sea Res.* 185 (March), 102229. <https://doi.org/10.1016/j.seares.2022.102229>.
- Vaissière, A.C., Levrel, H., Pioch, S., Carlier, A., 2014. Biodiversity offsets for offshore wind farm projects: the current situation in Europe. *Mar. Policy* 48, 172–183. <https://doi.org/10.1016/j.marpol.2014.03.023>.
- Van Colen, C., Thrush, S.F., Vincx, M., Ysebaert, T., 2013. Conditional responses of benthic communities to interference from an intertidal bivalve. *PLoS One* 8 (6), e65861. <https://doi.org/10.1371/journal.pone.0065861>.
- Villéger, S., Mason, N.W.H., Mouillot, D., 2008. New multidimensional functional diversity indices for a multifaceted framework in functional ecology. *Ecology* 89 (8), 2290–2301. <https://doi.org/10.1890/07-1206.1>.
- Vivier, B., Dauvin, J.C., Navon, M., Rusig, A.M., Mussio, I., Orvain, F., Boutouil, M., Claquin, P., 2021. Marine artificial reefs, a meta-analysis of their design, objectives and effectiveness. *Glob. Ecol. Conserv.* 27, e01538. <https://doi.org/10.1016/j.gecco.2021.e01538>.
- Voet, H.E.E., Vlaminck, E., Van Colen, C., Bodé, S., Boeckx, P., Degraer, S., Moens, T., Vanaverbeke, J., Braeckman, U., 2023. Organic matter processing in a [simulated] offshore wind farm ecosystem in current and future climate and aquaculture scenarios. *Sci. Total Environ.* 857 (October 2022). <https://doi.org/10.1016/j.scitotenv.2022.159285>.
- Wang, Y., Naumann, U., Wright, S.T., Warton, D.I., 2012. Mvabund- an R package for model-based analysis of multivariate abundance data. *Methods Ecol. Evol.* 3 (3), 471–474. <https://doi.org/10.1111/j.2041-210X.2012.00190.x>.
- Wrede, A., Andresen, H., Asmus, R., Wiltshire, K., Brey, T., 2019. Macrofaunal irrigation traits enhance predictability of nutrient fluxes across the sediment–water interface. *Mar. Ecol. Prog. Ser.* 632, 27–42. <https://doi.org/10.3354/meps13165>.
- Wright, S.W., Jeffrey, S.W., 1997. High-resolution HPLC system for chlorophylls and carotenoids of marine phytoplankton. In: Jeffrey, S.W., Mantoura, R.F.C., Wright, S.W. (Eds.), *Phytoplankton Pigments in Oceanography: Guidelines to Modern Methods*. UNESCO, Paris, p. 327e341.
- Zintzen, V., Norro, A., Massin, C., Mallefet, J., 2008. Spatial variability of epifaunal communities from artificial habitat: shipwrecks in the southern bight of the North Sea. *Estuar. Coast. Shelf Sci.* 76 (2), 327–344. <https://doi.org/10.1016/j.ecss.2007.07.012>.
- Zucco, C., May, V., Lüning, K., Shields, M.A., Payne, A.I.L., 2006. Influence of artificial hard substrata on benthic communities in the North Sea. In: *Marine Benthic Habitat Mapping. Proceedings of the First International Workshop*, Galway, Ireland, 2006. Joint Nature Conservation Committee (JNCC), Peterborough, UK.
- Zupan, M., Rumes, B., Vanaverbeke, J., Degraer, S., Kerckhof, F., 2023. Long-term succession on offshore wind farms and the role of species interactions. *Diversity* 15 (2), 1–23. <https://doi.org/10.3390/d15020288>.